CHAPTER: IV

DEVELOPMENT, CHARACTERIZATION AND POTENTIAL PERSPECTIVE OF POLY (VINYL ALCOHOL)/GRAPHENE OXIDE NANOCOMPOSITE FILMS

4.1. Introduction

Plastic packaging has been extensively utilized in the food sector for almost fifty years due to its functional, inexpensive, lightweight, and extremely versatile characteristics [1]. In response to growing environmental concerns related to the technologically advanced society, bio-based polymers have become a major focus of research in materials science [2]. Bioplastics have been used in many different types of commercial products, including disposable cutlery, medical devices, electronic equipment, and food packaging [3]. Researchers have focused to develop biodegradable polymers for packaging applications with efficient barrier, mechanical, optical, anti-microbial, and thermal properties to extend food product shelf life [4]. Thermoplastics account for the majority of plastics used in packaging applications because it can be economically formed into desired shapes, flexible in recycling, and can carry out packaging functions as well [5]. Polyolefins (high-density or low-density polypropylene, polyethylene, etc.), polyester, polystyrene, polycarbonates, vinyl polymers, nylon, etc. are the important constituent of thermoplastics in packaging [6].

Polyvinyl alcohol (PVA) is one of the few water-soluble vinyl polymer matrices that biodegrade with microorganisms and has also been accepted as generally recognized as a safe (GRAS) polymer by Food and Drug Administration-FDA for packaging [7, 8]. PVA-based material has diverse applications in the packaging sector such as coating of different types of films, layers in reinforced composite, food supplements coating agents, membrane separation, cosmetics and pharmaceuticals, paper, and textile industry as well as in medical applications [9]. However, PVA polymer films have some drawbacks, including a low tensile strength (TS), a high degree of water solubility, and low light barrier properties [10].

To overcome the limitations of neat PVA polymers, the addition of nanomaterials

into polymer chemistry has created a new avenue to improve the attributes of plastic materials [11]. Various nanostructured materials like silica, organoclay, clay, polysaccharide, carbon nanotube, graphene, nanocrystals, cellulose-based nanomaterials, metal and metal oxide nanomaterials such as Zn, Ti, colloidal Cu, Ag, Au, Zn, ZnO, TiO_2, SiO_2, MgO, etc. have been researched extensively as fillers in a wide range of packaging application [12]. However, nanotechnology has advanced significantly after the discovery of graphene and its derivatives due to its higher functional properties with polymer matrix [13]. For graphene and its functionalized derivatives like graphene oxide (GO), a stable aqueous colloidal dispersion and large interplanar space allow GO to exfoliate in polar solvent [14]. Typically, to achieve a notable improvement in the overall efficiency of graphene and its derivatives, higher interfacial bonding and homogenized dispersion of nanofillers with polymer matrix are necessary [15]. Dispersion of GO in polar protic/aprotic solvents with notable amounts of water-soluble organic molecules, like PVA would be a feasible approach towards the fabrication of particulate nanocomposite (NC) due to the existence of hydrogen attracting oxygen functional groups in GO [16]. Moreover, the mechanical properties of NC film experience a gradual deterioration as the concentration of GO increases, while a significant enhancement of mechanical properties was observed with a change in the molecular weight of the polymer [17].

Thus, the present chapter is aimed to improve the properties of PVA films by adding GO nanofiller, as well as to investigate the effect of GO nanofiller concentrations on PVA/GO nanocomposite films. A comprehensive understanding of the experimental work was achieved by through discussion and validation of the findings with previous research, highlighting its potential applications in packaging.

4.2 Experimental procedure

4.2.1 Development of PVA and PVA/GO films

The materials and reagents used for the development of films are discussed in detailed in Chapter 3, under the materials and methodology section 3.1. The development of films has been done via solution casting technique. Initially, 3 wt.% (3 g) of PVA has been dissolved in 100 ml of distilled water to develop a neat PVA solution. Thereafter, the solution was stirred in a magnetic stirrer for 3 h at 90 ℃ and 600 rpm for homogeneous mixing of PVA [18,19]. Different concentrations 0.1 wt.%-0.7 wt.% (0.1g to 0.7g) of GO nanofillers were added into the PVA solution and stirred continuously for 2 h for uniform dispersion of GO.

As a plasticizer, 1% (v/v) glycerol (1 ml) was then added to the PVA/GO solution and stirred for 15 min. The solution was then sonicated for 30 min to ensure all the air bubbles present in the solution were completely removed. A 2% (v/v) $CaCl_2$ (2ml) solution was poured onto the petri plates for effective crosslinking of the NC films [20]. After that, 50 ml of the sonicated PVA/GO solution was poured onto the petri plates, and placed in a hot air oven at a temperature range between 45 ℃ to 50 ℃ for 24 h to 30 h. Finally, the dried films have been peeled off and kept in a desiccator to prevent moisture absorption.

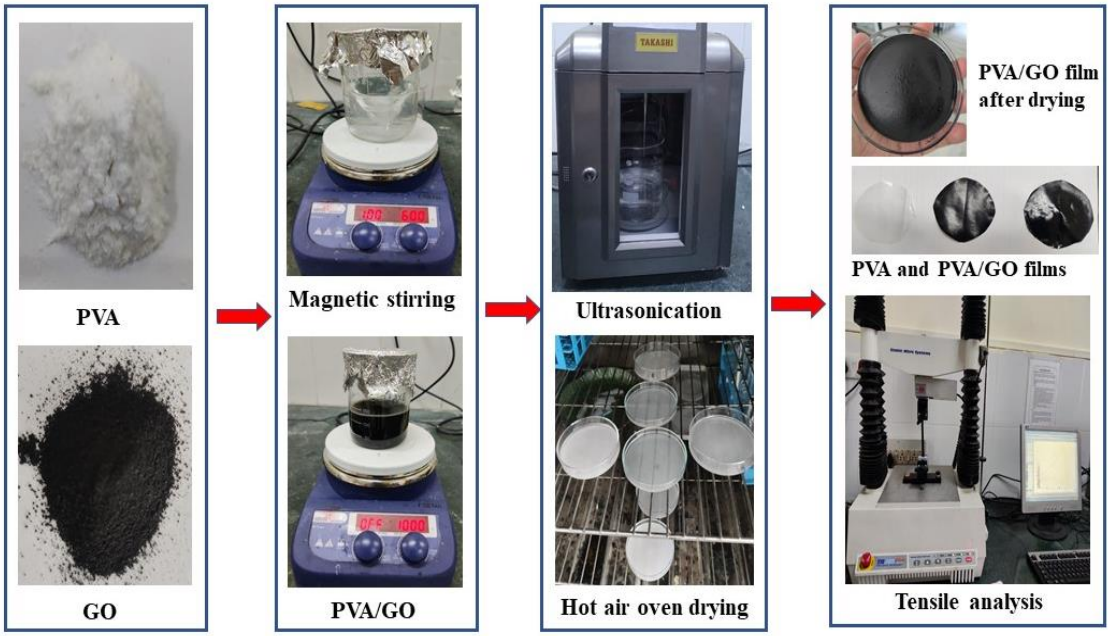

Figure 4.1. Schematic diagram showing the fabrication of nanocomposite film

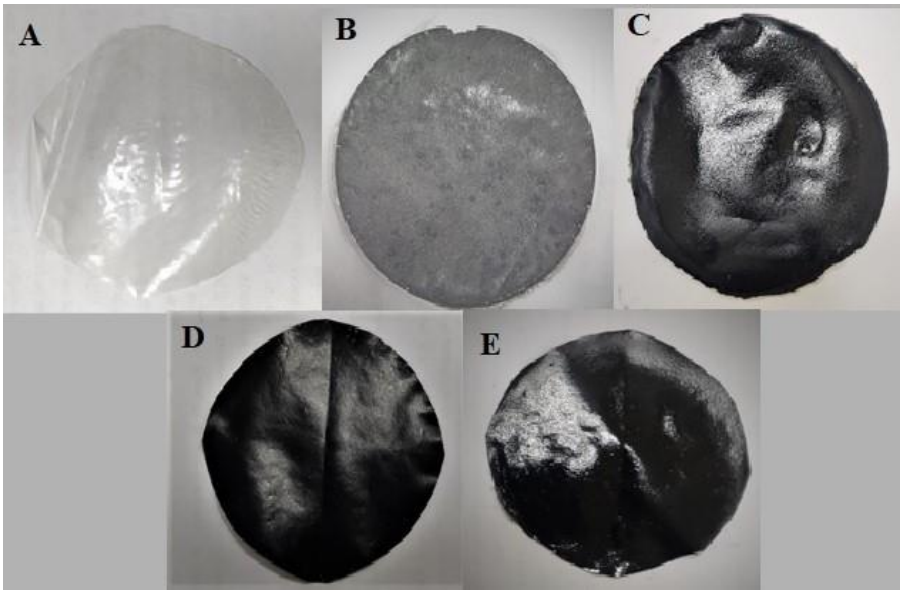

Figure 4.2 PVA-based films with varying concentrations of GO **(A)** Neat PVA **(B)** PVA+GO (0.1%) **(C)** PVA+GO (0.3%) **(D)** PVA+GO (0.5 %) **(E)** PVA+GO (0.7%)

Figure 4.1 shows the schematic steps for the fabrication of nanocomposite films by solvent casting method. Figure 4.2. shows different compositions of PVA and PVA/GO developed films.

4.3 Results and discussion

Different physical, chemical, mechanical, morphological, barrier, thermal, and water vapor permeability antimicrobial and biodegradable properties of the films were discussed and validated with published research to understand the effect of GO nano-filler in PVA polymer.

4.3.1 Determination of film's thickness, tensile properties, and morphological study

The thickness, TS, and elongation at break (EAB) of the developed films were evaluated and summarised in Table 4.1. It was found that the thickness of the developed films varied from 0.79 mm to 0.86 mm. The inclusion of solid nanoparticles in PVA films caused a marginal increment in the thickness of the NC films as compared to neat PVA film. This suggests that the addition of solid nanoparticles in the NC films had an impact on their physical properties. Moreover, the properties of the NC films were affected by various factors, such as the interactions between the polymer and nanofillers, the concentration of fillers, the morphology of the distribution, and the size and geometry of the fillers [21].

Table 4.1 Thickness, and tensile properties of the developed films

Films	PVA wt.%	GO wt. %	Film thickness (mm)	Tensile Strength (MPa)	Elongation at break (%)
A	3	0	0.79 ± 0.013^{a}	1.40 ± 0.023^{a}	325.54 ± 5.41^{a}
B	3	0.1	0.83 ± 0.007^{b}	1.43 ± 0.008^{a}	201.02 ± 5.10^{b}
C	3	0.3	0.83 ± 0.005^{b}	1.51 ± 0.039^{b}	268.64 ± 5.82^{c}
D	3	0.5	0.84 ± 0.005^{b}	1.73 ± 0.017^{c}	141.74 ± 3.63^{d}
E	3	0.7	0.86 ± 0.006^{c}	1.99 ± 0.024^{d}	115.58 ± 3.92^{e}

Data was expressed as Mean ± SD of triplicate assays. The corresponding column's letters (a-e) differ significantly ($P \leq 0.05$).

It was observed from Table 4.1 that the TS of the films was significantly enhanced from 1.40±0.023 MPa to 1.99±0.024 MPa ($P \leq 0.05$) with the addition of GO. The improvement in TS was attributed to the homogenized dispersion and strong interfacial interaction, due to the formation of H-bonds between the polymer chain and GO surface. The addition of GO resulted in a uniform dispersion of the filler, which led to better load transfer and higher

TS compared to PVA film. The % EAB of the films ranged between 115.58% to 325.54%, as shown in Table 4.1. The EAB was increased significantly from 201.02% to 268.64% as the concentration of GO increased from 0.1 wt.% to 0.3 wt.%. However, it was decreased significantly with further addition of GO from 0.3 wt.% to 0.7 wt.%. This phenomenon is attributed to the inadequate dispersion of nanofillers within the polymer matrix when its concentration exceeds the optimal level. The resulting nanoparticle aggregation imparts brittleness to the nanocomposite film which subsequently lowers the %EAB. Thus, addition of GO in PVA resulted in the improvement of tensile properties, which is attributed to the strong interfacial interaction, optimum concentration and homogenized dispersion of the GO nanofiller. A similar trend of TS and % EAB was observed for PVA/GO film, in which the EAB was 211% at 0.08% GO concentration and concluded that the reduction in EAB was due to the film's brittle nature after the intercalation of nanofillers [22].

For SEM micrographs 0.3 wt.% GO concentration PVA/GO film is considered because of improved EAB and WVP among the developed NC films The SEM micrograph in Figure 4.3 (a) revealed uniform dispersion of GO nanofillers in the PVA polymer, which resulted in fewer surface defects.

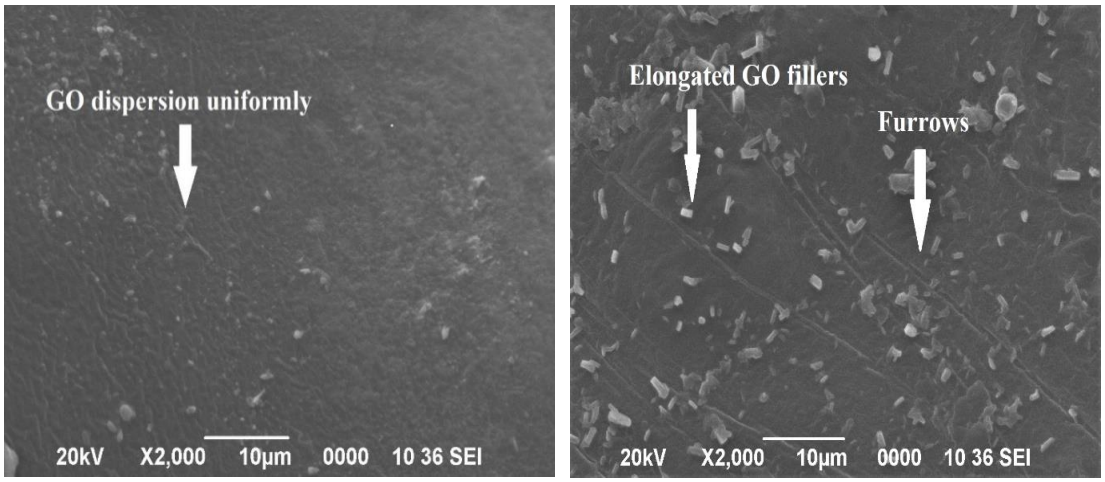

(a) Before the tensile test (b) After tensile test

Figure 4.3 SEM image of PVA/GO at 0.3% of GO **(a)** before and **(b)** after the tensile test

Figure 4.3 (b) SEM micrograph showed the formation of furrows on the surface of the film, which was due to the elongation effect of PVA/GO in the tensile direction. In addition, it was observed that the nanofillers reach their maximum length with the polymer matrix before the rupture of film. This confirmed that GO adheres strongly with PVA

polymer, which leads to an increase in the strength of the PVA/GO film under loading conditions.

4.3.2 Film's color, UV-Vis light absorbance, and opacity

The color parameters of developed films were shown in Table 4.2. It was noticed that the color of the films varied significantly ($P \leq 0.05$) with the addition of GO. The measured values of L*, a*, and b* were ranged from 31.98 to 88.38, -0.48 to 2.91, and 2.2 to -1.53, respectively. It was observed that film 'A' showed the lightest tint among all the developed films. However, the lightness of the films diminished as the GO concentration enhanced from 0.1 wt.% to 0.7 wt.%. Film 'E' showed the lowest L^* value as compared to film 'A'. Similarly, film 'A' had a negative value of a^* which refers to a slight greenish tint of PVA film. However, with the addition of GO, the value of a^* was shifted towards the positive side. It was also seen that film 'A' and 'B' showed the positive value of b^* which referred to the yellowish tint. From films 'C' to 'E', the value of b^* was increased which relate to bluish color of the films. Thus, the results showed that incorporation of GO nanofiller significantly modifies the color of the films to darker side at higher concentrations.

Table 4.2 Film's color, and barrier properties

Films	Color			Opacity	%MRC	WVP×10^{-5} (g/m.hr. Pa)
	L^*	a^*	b^*			
A	88.38± 0.23^{a}	-0.48± 0.02^{a}	2.2± 0.030^{a}	0.30± 0.004^{a}	79.33± 0.27^{a}	8.16± 0.08^{a}
B	42.65± 0.63^{b}	0.89± 0.02^{b}	1.59± 0.050^{b}	0.84± 0.016^{b}	80.08± 0.06^{b}	7.25± 0.09^{b}
C	36.11± 0.44^{c}	1.79± 0.04^{c}	-1.23± 0.131^{c}	2.07± 0.013^{c}	81.06± 0.05^{c}	6.76± 0.06^{c}
D	34.68± 0.20^{d}	2.16± 0.01^{d}	-1.46± 0.006^{d}	2.79± 0.005^{d}	81.74± 0.23^{d}	6.69± 0.08^{cd}
E	31.98± 0.12^{e}	2.91± 0.04^{e}	-1.53± 0.025^{e}	3.21± 0.034^{e}	82.06± 0.06^{e}	6.88± 0.04^{d}

Data was expressed as Mean ± SD of triplicate assays. The corresponding column's letters (a-e) differ significantly ($P \leq 0.05$).

For food packaging classifications, the light barrier property of packaging film is an important design feature for certain food packaging classifications, as exposure to light can cause food spoilage, oxidation, and degradation of nutrients. The UV-Vis absorption spectra shown in Figure 4.4 indicates the light absorption property of the films at various wavelengths. The absorption spectra showed that the developed films had a significant light

absorption in the UV wavelength range. Among them, film 'A' had the least light absorption in the UV range. However, the absorbance was increased significantly from film

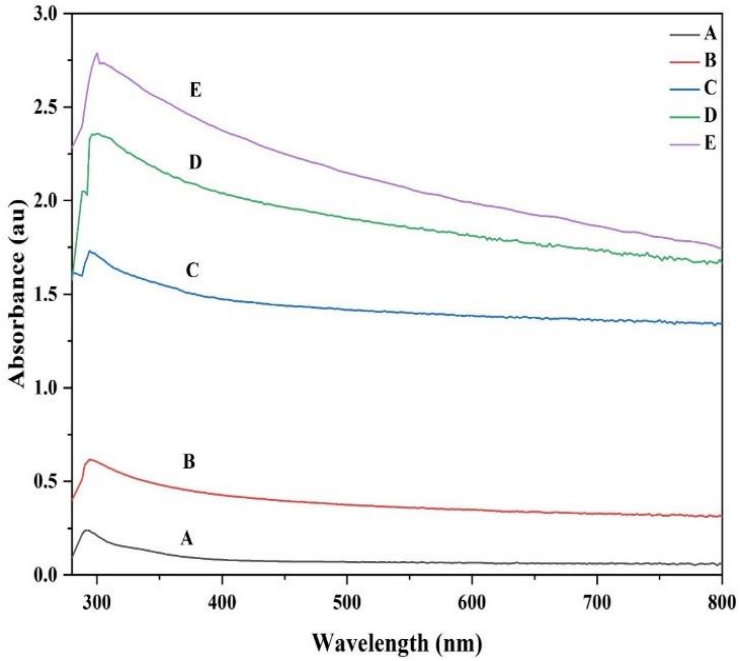

Figure 4.4 UV-Vis light absorbance of PVA and PVA/GO films

'B' to 'E', as the concentration of GO was increased. It was observed from the figure 4.4 that a distinctive absorbance peak had appeared at a wavelength close to 300 nm which is due to the transition of C=O. The transparency of a film was determined by its opacity value where less transparency is related to higher opaque material. The opacity values of developed films were tabulated in Table 4.2. The opacity of the films varied significantly from 0.30 to 3.21 ($P \leq 0.05$). From film 'B' to 'E', the opacity was increased from 181.57% to 967.10% with respect to film 'A'. The improved opacity indicates a better light barrier nature of PVA/GO films compared to neat PVA film. Similar results were reported for ZnO, and GO nanofiller in different polymer composites [23,24]. Thus, addition of GO nanofillers significantly improves the UV-light barrier capabilities of PVA film, eliminating its disadvantages in terms of barrier properties.

4.3.3 Thermal analysis

The DSC thermograms of PVA and PVA/GO nanocomposite films are shown in Figure 4.5. The values of glass transition temperature (T_g), melting temperature (T_m), enthalpy of pure PVA crystal (ΔH_m) and % crystallinity ($\%X_c$) of the developed samples has been determined and summarised in Table 4.3. It was observed that the *Tg* of PVA was

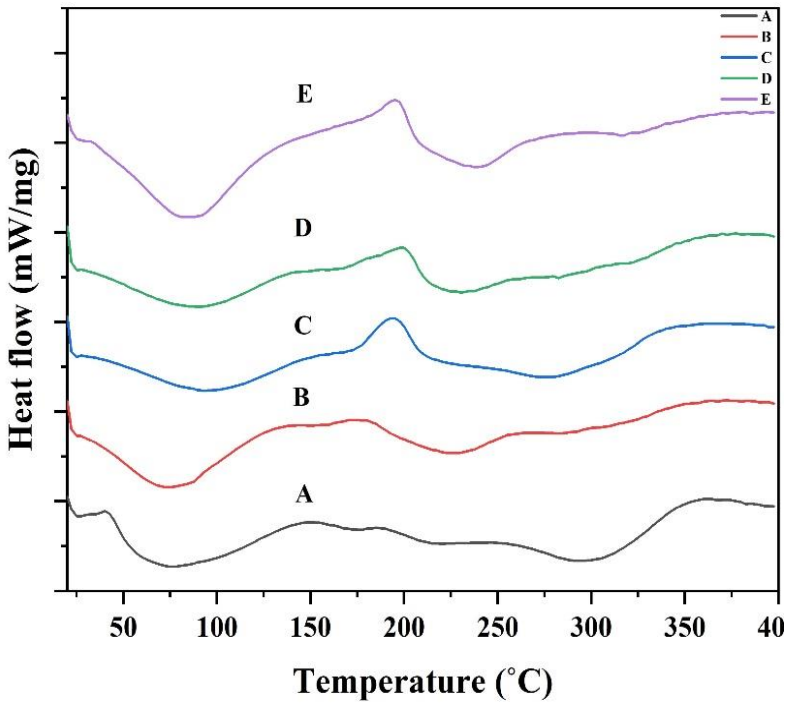

Figure 4.5 DSC analysis of PVA and PVA/GO films

approximately 72.03 ℃. However, with the incorporation of GO from 0.1 wt.%-0.7 wt.%, a significant increment in T_g was seen. From the DSC result it was observed that the highest T_g was achieved at 0.3 wt.% GO, with a value of 95.62 °C. This finding revealed that addition of GO had a greater impact on the mobility of PVA chains. The oxygen-containing functional groups of GO formed strong H-bonds with the -OH groups of PVA chains, resulting in the obstruction of PVA chain movement which results in the increment of T_g [25]. The DSC endotherm curve of PVA film observed at 212 °C indicates the occurrence of melting. This was evidenced by the simultaneous softening and fusion of the polymer particles into more visually transparent mass. Similar to T_g, a significant increment in T_m was also observed with the addition of GO, as seen in Table 4.3. The T_m was increased from 220.04 °C to 275.54 °C at 0.3 wt.% GO. The observed elevation in T_m can be attributed to the thermal insulating properties exhibited by the addition of nano fillers, that are uniformly distributed across the polymer chain. This phenomenon significantly influences the melting characteristics of the polymer NCs. However above 0.3 wt.% GO content, the T_m of the NC films was declined which could be attributed to two factors i.e. the quantity of nanofillers present and the level of dispersion achieved [26]. An excessive quantity of filler in polymer matrix results in inadequate dispersion within the matrix. Consequently, the filler particles agglomerate, leading to a reduction in the thermal properties [27]. From the DSC thermograms, the observed shape and area of the melting endotherm curve corresponds to

the varying degrees of crystallinity detected in samples.

Table 4.3 Thermal properties of PVA and PVA/GO films

Sample	T_g (℃)	T_m (℃)	ΔH_m(J/g)	$\%X_c$
A	72.03	220.04	26.65	17.08
B	72.41	227.53	30.32	19.44
C	95.62	275.54	50.28	32.23
D	87.95	232.53	41.31	26.48
E	84.70	235.03	38.34	24.56

The crystallinity degree of the samples is tabulated in Table 4.3, where $\Delta H°_m$ is the heat required for melting 100% crystalline PVA i.e. 156 (J/g) [26]. As seen in Table 4.3, the $\%X_c$ of PVA film is approximately 17.08%, which was further enhanced with the addition of GO. The $\%X_c$ was increased to 32.32% for 0.3 wt.% GO and thereafter decreases with further increment in GO concentration. The change in the $\%X_c$ may be attributed to the interaction between PVA and GO nanofiller in the amorphous phase, leading to a disruption in the crystal structure and thus reducing the enthalpy associated with the phase transition [28]. Similar observation of melting enthalpy of GO based nanocomposites has also been observed in earlier studies which validates that addition of GO improves the thermal stability of polymers [26].

The thermal degradation properties of the developed films were evaluated by thermogravimetric analysis (TGA). Figures 4.6 (a) and (b) depicts the TGA and DTG curves of the fabricated films up to 600 ℃. The TGA and DTG thermographs demonstrate the mass loss percentage and rate of mass loss over a given range of temperatures. From Figure 4.6(a), a three stages mass degradation of PVA polymer and its corresponding PVA/GO NC films were observed. It was seen that an initial 10% mass loss at a temperature range between 30 ℃ to 150 ℃ was due to the evaporation of moisture present in the polymer film structure [19]. The second and third stage mass loss was approximately 50%-60% and 20%-30%, corresponding to the degradation of the adjacent and main chain of the PVA structure followed by the formation of polyene [29]. From Figure 4.6(a), it was observed that the onset temperature for second and third stage of mass degradation of PVA/GO film was approximately at 250 ℃ and 400 ℃ respectively. The degradation temperature of the NC films was significantly enhanced with the addition of GO. The sp^2-hybridized carbon structure and high specific surface area of GO forms H-bonds with PVA due to the presence of oxygen-containing functional groups on its surface. During

pyrolysis, the composite material undergoes thermal degradation resulting in the release of volatile products. However, due to the H-bonding between GO and PVA, a higher amount of heat is required to break the linkage, which slows down the degradation process of the volatile products. This leads to a reduction in pyrolysis and overall degradation of the material. Thus, PVA/GO NC materials provides improved thermal stability and reduced pyrolysis behaviour compared to pure PVA materials.

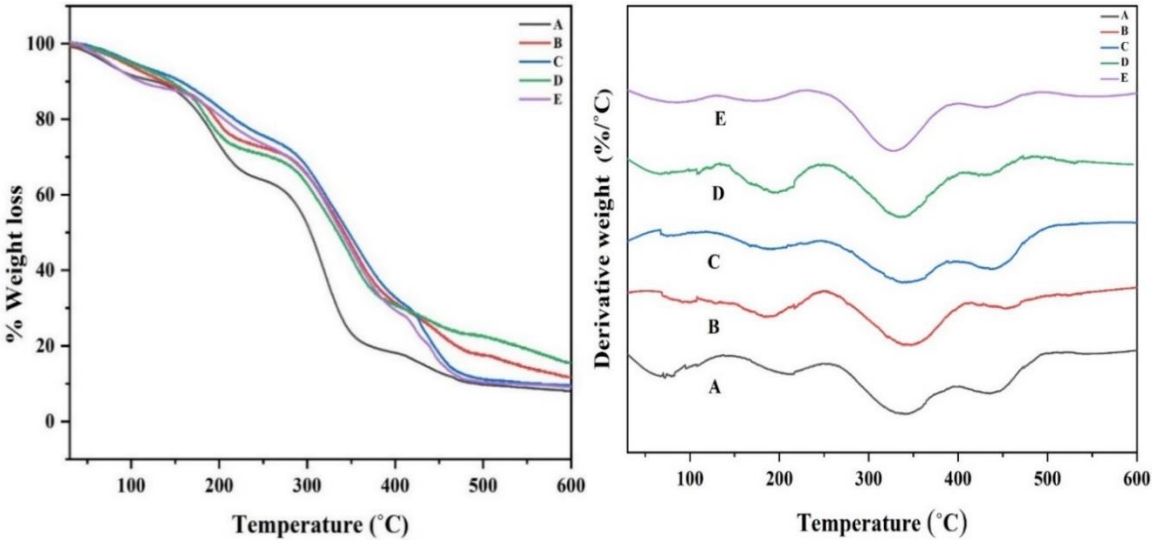

(a) TGA **(b)** DTG

Figure 4.6 (a) TGA and **(b)** DTG thermographs of PVA and PVA/GO films

The DTG plot evaluates the rate of mass loss in a given temperature range, and three-stage decomposition peaks were observed for all the developed films as shown in Figure 4.6(b). The first stage of decomposition occurred in a temperature range of 40 ℃-150 ℃, and resulted in a mass loss of 5%-15%. The second stage of degradation, which accounted for approximately 50%-60% of the mass loss, occurred at an onset temperature of 250 °C. The final decomposition of the films occurred at a temperature above 400 °C, with a mass loss of approximately 25%-30%. The onset temperature for maximum mass loss of PVA/GO films was in the temperature range of 250 ℃–370 ℃, which was 12%–15% higher than the onset temperature of neat PVA film. This confirmed that the addition of GO in PVA films enhanced their thermal stability, minimizing the dehydration reaction and mass loss during pyrolysis. The higher thermal stability of GO increases the onset temperature of the polymer, which leads to an increase resistance to heat exposure. A similar trend in the DTG plot was observed for PVA/GO films with 0.5 wt.% GO, where

the second stage degradation for 50% mass loss occurred in a temperature range between 338 ℃-358 ℃, which validates the present work [30].

4.3.4 Moisture retention capacity, water vapor permeability, solubility and swelling

The MRC and WVP play a vital role in preserving the quality and shelf life of packaged food in long term to control the migration of moisture from the films. MRC is the ability of a film to retain moisture and films with a high MRC are suitable for packaging applications [19]. The MRC of the developed films was ranged from 79.33% to 82.06% as seen in Figure 4.7. Film 'A' had the least MRC, whereas a significant increment in MRC was observed from film 'B' to 'E'. The higher MRC of PVA/GO films was due to the hydrophilic nature of PVA, and GO which leads to the retention of water molecules within the matrix and allows them to establish a H-bond. This reduces the polymer chain mobility and diffusion of water molecules within the film. The reduction in crystallinity of PVA/GO films also shows high MRC due to the free amorphous region in the films [30]. As reported in previous studies, the recommended range of MRC for food packaging films is 78-95% [10]. This suggests that the MRC of developed PVA/GO film falls within the recommended range of food packaging applications and have the potential to retain moisture and prevent moisture loss, to preserve the quality and shelf life of the packaged food.

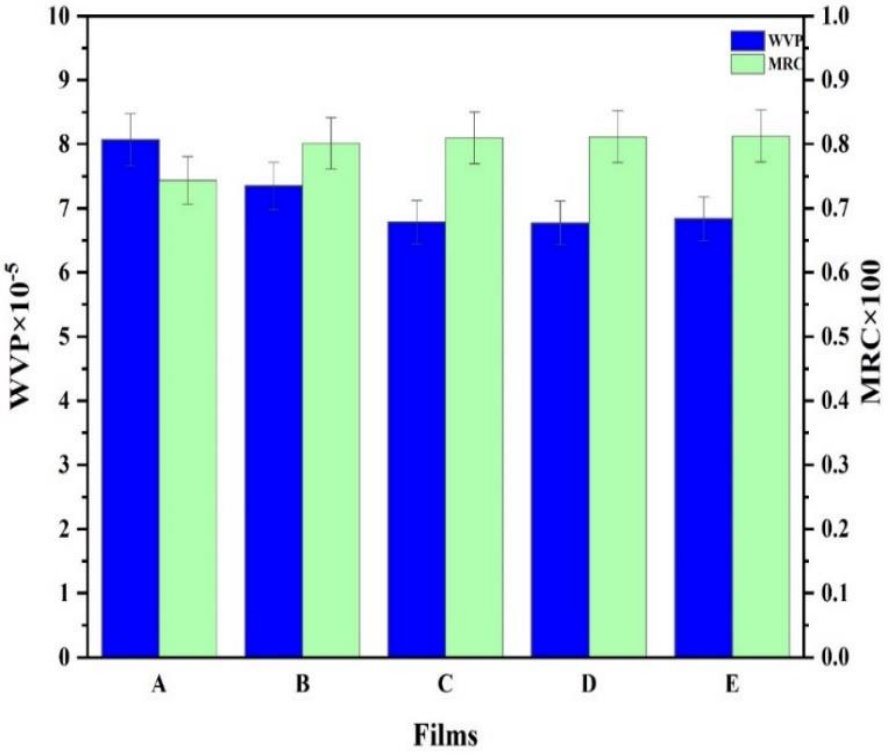

Figure 4.7 MRC and WVP of PVA and PVA/GO films

The water resistant of a film and ability of a film to trap water molecules are determined by film's solubility and swelling capability. It was observed that within 4-5 hours the dissolution of films in water was observed. A similar observation was observed for PVA based films in which the films were completely dissolved in water [31].

The WVP is a crucial parameter in packaging because it directly impacts the food quality contained in it [30]. The WVP values of the films, presented in Figure 4.7, ranged from $8.16\pm0.08\times10^{-5}$ to $6.88\pm0.04\times10^{-5}$ (g/m.hr.Pa). A reduction in WVP by 11.15% to 18.01% was observed for films 'B' to 'D' (0.1–0.5% GO) compared to film 'A'. However, for film 'E', the WVP increased by 2.84% with further addition of GO. The increase in WVP is attributed to the agglomeration of nanofillers at higher loadings, which generate micro-voids and interfacial defects, offering easier diffusion pathways for water vapor, thereby lowering the barrier performance of the films. Conversely, at concentrations below the optimum level, uniform GO dispersion decreases the hydroxyl group availability and polymer chain mobility, while enhancing the tortuosity of diffusion pathways for water molecules, ultimately improving the barrier properties of the nanocomposite films. The results obtained in this work are consistent with earlier reports, and the values achieved showed an improvement over those reported in the literature.

Table 4.4 Comparison table of previous literature with the present study

Polymer	**Additives**	**TS (Mpa)**	**% EAB**	**WVP×10^{-5} (g/m.hr.Pa)**	***Tg*** **(℃)**	**Refrences**
PHBV	CNC/GO	26	13	8.28	78.9	[32]
CS-PVP	GO	-	-	0.81	65	[33]
PVA	Au	1.45	34.79	-	-	[34]
PVA	GO	1.51	96.97	-	-	[34]
PVA	GO (0.3%)	1.51	268.64	6.76	95.62	Present study

4.3.5 FTIR analysis

FTIR analysis was carried out to determine the structural characteristics as well as to recognize the presence of significant chemical groups and their bonding in a polymer matrix. The FTIR spectra of the developed films has been shown in Figure 4.8. It was observed that neat PVA films showed large absorption peak that extends between 3200 cm^{-1} to 3700 cm^{-1} which is due to -OH symmetric stretching and vibration. The appearance in

the absorbance peak at 1033 cm^{-1}, 1382 cm^{-1}, 1466 cm^{-1}, 1645 cm^{-1}, 2927 cm^{-1} and 3431 cm^{-1} corresponds to C-O stretch, C-H vibration, C-H bending of CH_2, H-O-H deformation, -CH_2 stretch and -OH stretching respectively [35].

The FTIR spectra of PVA/GO films showed a minimum effect on the structure of PVA. However, for a complicated polymer blend process with nanofillers, the configurations, and interactions like H-bonding predict the thermal, and electrical properties of polymer NCs. For PVA/GO NC film, the absorption peak of -OH stretching shifts to a lower wavenumber while adding GO in PVA. From figure 4.8, it can be observed that the absorbance peak has been reduced from 3422 cm^{-1} to 3403 cm^{-1}, by the addition of GO from 0.1 wt.% to 0.7 wt.%. When GO is added to PVA, the H-bond in the -OH of the PVA dissociates and forms an additional H-bond with the functional group of GO containing oxygen which is thermodynamically more favourable. The increase in the concentration of GO nanofiller resulted in H-bond degradation in the -OH groups of the PVA polymer chain due to increase in conductivity, thus forming an additional H-bond with GO which is an important factor for characteristic intensification [36]. This shows that the introduction of GO in the PVA/GO NC polymer system has good interaction with PVA which therefore enhances the amorphousness and thermal stability of the NC films.

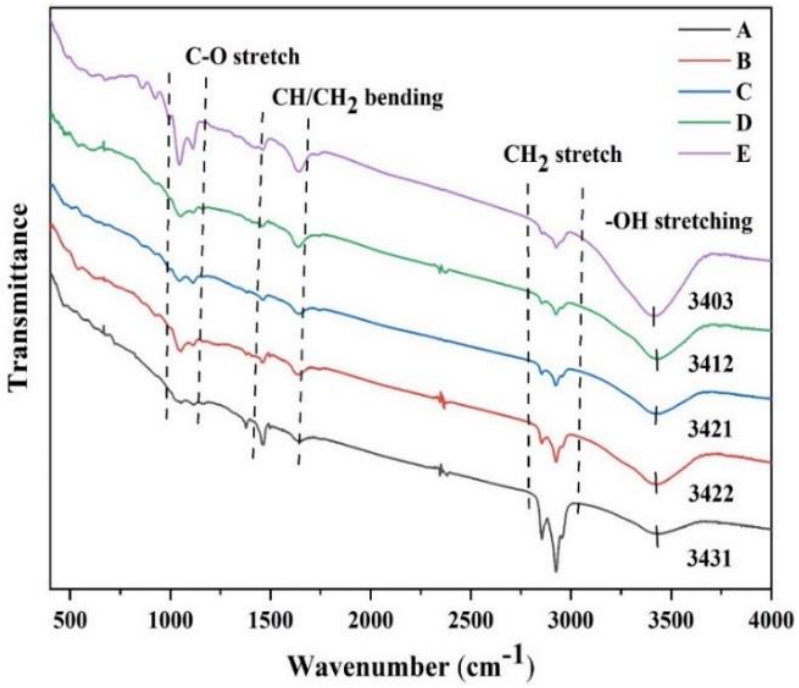

Figure 4.8 FTIR analysis of PVA and PVA/GO films

4.3.6 Antimicrobial properties

The antimicrobial property of packing material is an important feature that should be considered in order to minimise the growth of microorganisms in food. An examination of the antibacterial activity of the films against gram-positive *S. aureus* and gram-negative *E. coli* bacteria was carried out based on the diameter of the inhibition zone. The antibacterial activity by disk diffusion method has been shown in figure 4.9. The inhibition zone diameter of the films is tabulated in Table 4.5. From figure 4.9 (a) and (b) it was observed that neat PVA film lacks antibacterial property with negative inhibition zones against both the bacteria. The NC films also exhibited no antibacterial effect against *E. coli* (gram-negative bacteria) as shown in Figure 4.9(a). However, addition of GO fillers showed the antibacterial activity against *S. aureus*. From figure 4.9(b) and (c), it was observed that the inhibition zone diameter was enhanced from 9 mm to 10.8 mm as the concentration of GO was increased from 0.1%-0.7% (B to E). This revealed that the presence of GO showed prominent antibacterial agents that creates a spectrum of inactivity in diverse samples.

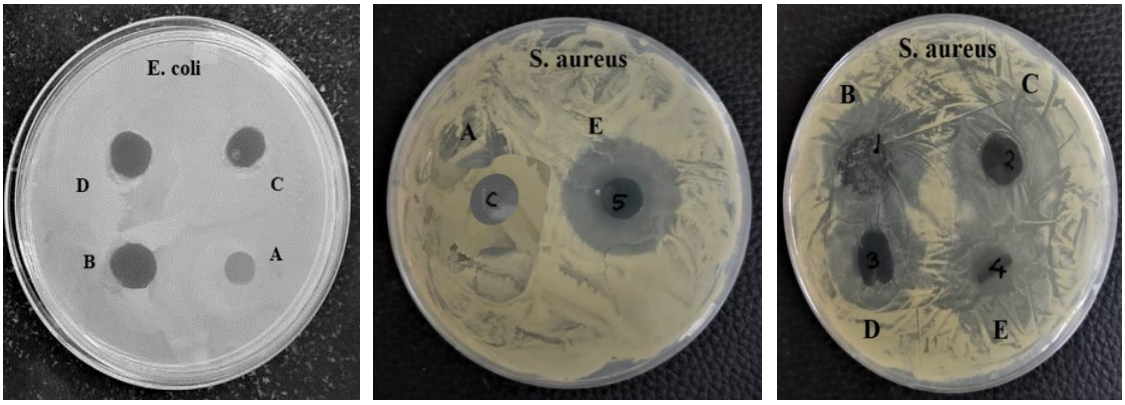

(a) (b) (c)

Figure 4.9 Antibacterial activity by disk diffusion method

Table 4.5 Inhibition zone diameter (mm)

Sample	*S. aureus* (mm)	*E. coli* (mm)
A	-	-
B	9.0±0.06	-
C	9.8±0.32	-
D	10.3±0.07	-
E	10.8±0.02	-

The reasons behind the inhibition of bacterial proliferation as mediated by GO nanoparticles are (i) physical interactions between GO fillers and bacteria cells through direct contact with the basal planes or sharp edges of the GO, (ii) generation of reactive

oxygen species (ROS) which induces the oxidative stress in bacteria, thereby damaging cellular components like proteins, lipids, and DNA, (iii) antibacterial adhesion property and ion release of GO fillers. Moreover, an exact mechanisms of bacterial growth inhibition by GO nanoparticles also vary depending on filler size, concentration, surface functionalization, and bacterial species [37,38,39]. Based on the analysis, it can be concluded that the developed PVA/GO films showed better antibacterial activity against *S. aureus* compared to neat PVA film when exposed to GO nanofillers. Similar findings were reported for PVA/GO/Ag nanocomposite films, which exhibited efficient antibacterial activity against *S. aureus* and *E. coli* despite the absence of inhibition zone around neat PVA film [37].

4.3.7 Biodegradation analysis

4.3.7.1 Microbial

The majority of microorganisms capable of decomposing PVA were discovered as aerobic bacteria from the genera *Pseudomonas, Alcaligenes, and Bacillus. Pseudomonas* species were the first bacteria to be found in soil samples that could use PVA as their only source of carbon [40]. Figure 4.10 depicts the biodegradability test on agar media using a modified ASTM G21-70 technique.

Two different types of bacteria strain i.e. *B. subtilis* and *P. putida* were used in this experiment. At day 0, there was an absence of *B. subtilis* and *P. putida* microbial growth on the bioplastic sample and agar media. On the day1, both the bacteria strains began to grow and covers the bioplastic surface. The microbial growth became evident on the bioplastic sample as it continues to proliferate and covers the surface on day 3. Moreover, the media used in the context consists of only minerals and lacks any supplementary carbon source. Consequently, the microbial growth could be attributed to the degradation of bioplastic surfaces for utilizing it as a source of carbon. Various enzyme systems have been discovered that facilitate the degradation of PVA. Within these enzyme systems, the primary carbon-carbon bonds of PVA are initially cleaved due to dehydrogenase or oxidase enzymes. Subsequently, this cleavage is succeeded by the action of hydrolase or aldolase enzymes. The PVA dehydrogenase, responsible for the degradation of PVA, has mostly been identified in various strains of Pseudomonas bacteria [41]. A comparison study was performed on synthetic plastic, where no growth was observed on negative control. The synthetic plastic exhibited a lack of nutritional value for the bacterial growth, indicating that it exhibits significant resistance qualities against microorganisms.

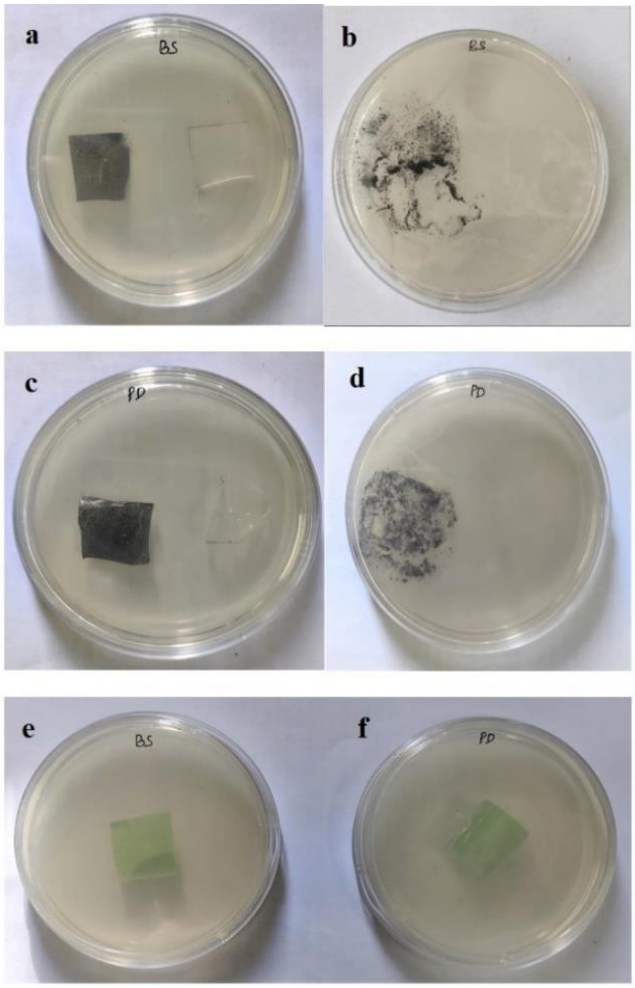

Figure 4.10 Biodegradation test of (a) *B. subtilis* day 0 (b) day 3, full degradation of film observed (c*) P. putida* day 0 (d) day 3, full degradation of film (e and f) negative control (synthetic plastic) on day 3

4.3.7.2 Soil burial

The results of the biodegradability assessment, performed using a soil burial test, is presented in figure 4.11. Figure 4.12 provides visual documentation of the entire experiment performed and the films used. The test result demonstrates a positive correlation between burial duration and weight loss of the bioplastic, suggesting a proportional increase in biodegradation. On 10^{th} day after burial, PVA film exhibited a weight loss of approximately 8.42%. However, as compared to PVA films, the deterioration of PVA/GO based films was apparently in between 1.93 % to 8.66 % as seen in Figure 4.11. After 20^{th} days, the weight reduction climbed to around 10.25% for PVA and 2.51 % to 10.67 % for PVA/GO films. During the degradation of PVA, the polymer chains were cleaved, resulting in a decrease in their molecular weight. The cleavage process initiated through enzymatic oxidation, specifically

targeting the hydroxyl and carbonyl groups present within the structure of PVA. As a result of the enzymatic processes, the PVA molecules became more sensitive to breakdown [42].

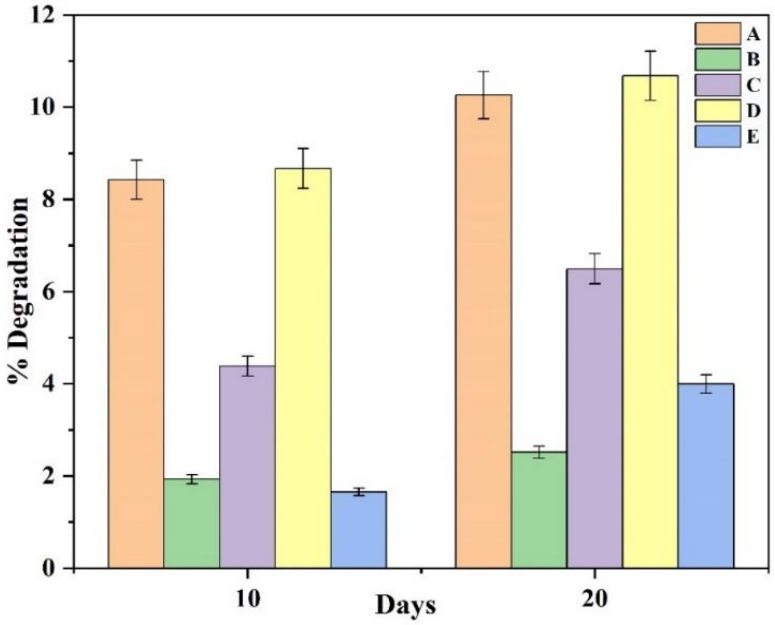

Figure 4.11 Soil burial degradation rate

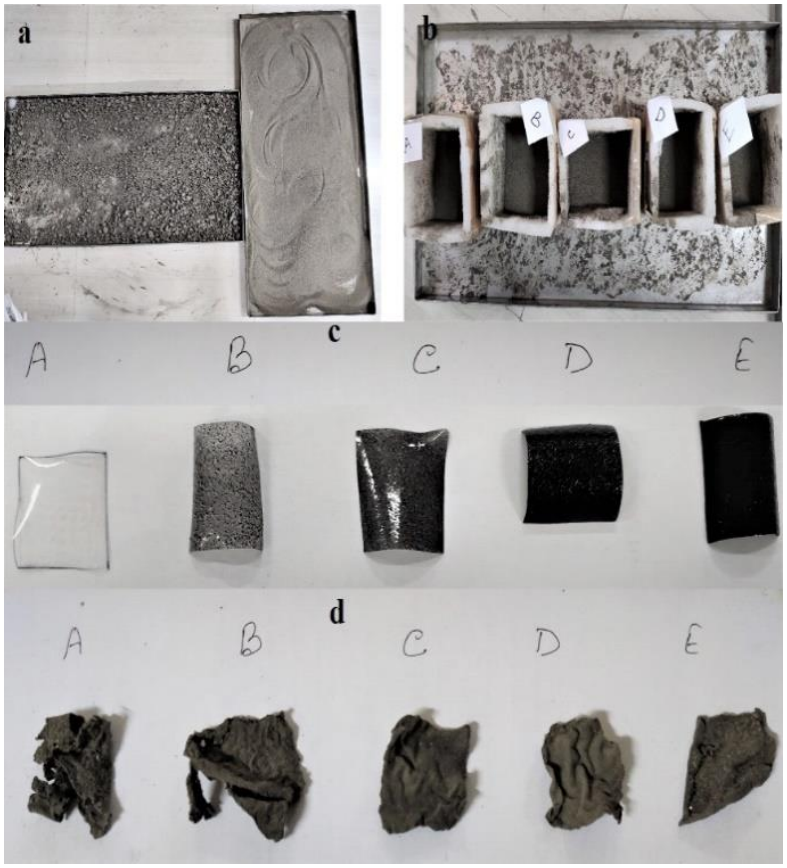

Figure 4.12 Soil burial analysis of PVA and PVA/GO films (a, b) soil preparation (c) samples (3×3 cm) (d) 20th day sample degradation

After 20 days, it was observed that the average degradation rate of PVA/GO films was approximately 46.5% lower as compared to neat PVA film. This reduction in degradation rate can be attributed to the formation of strong H bond interactions of GO with the polymeric phase. These interactions increased the nanocomposite's overall stability. The result demonstrates effective dispersion of GO within the polymeric matrix and formation of strong intermolecular linkages between fillers and matrix which subsequently increase its mechanical properties [43]. A similar observation was noticed for PVA-based films which showed 27.50% reduction in mass degradation rate after incorporation of nanofillers [41]. These findings underscore the potential of PVA-based bioplastics, especially when modified with nanofillers like GO, as environmentally friendly alternatives to traditional plastics. Further research in this direction holds promise for addressing plastic pollution and advancing sustainable materials.

4.4 Conclusions

In the present study PVA based NC films were developed by incorporating GO at different concentrations (0.1%-0.7%). The effect of GO on essential properties of the hybrid films such as physiochemical, mechanical, barrier, optical, thermal, morphological, antimicrobial, and biodegradation properties was observed. Some important findings from the present research work are as follows:

- The incorporation of GO nanoparticles into the PVA polymer resulted in a significant increase in the thickness of NC films. Among the fabricated films, a notable improvement in tensile strength and elongation at break was observed at a 0.3% GO concentration. Additionally, SEM micrographs showed uniform dispersion of GO, minimal surface defects and reduced agglomeration in the PVA/GO NC film.
- The light barrier properties of PVA/GO films showed higher absorbance at UV wavelength. The opacity of the PVA/GO films was increased while enhancing the GO concentration with respect to neat PVA.
- DSC analysis revealed an increase in glass transition and melting temperatures, along with alterations in crystallinity. This was attributed to enhanced crosslinking between PVA and GO, demonstrating its potential for modifying the thermal properties of the developed nanocomposite films. TGA and DTG graphs also showed a significant enhancement in the decomposition temperature of PVA/GO

films with minimum mass loss as compared to PVA film.

- A significant reduction in WVP and adequate MRC of PVA/GO films was observed compared to PVA film showcasing its improved barrier properties.
- FTIR spectra confirmed that incorporation of GO leads to strong H-bond within the polymer blend that significantly enhances the amorphousness and thermal stability of the NC films.
- Antimicrobial analysis showed PVA/GO films had excellent antibacterial properties against *S. aureus* bacteria. However, there was no antibacterial activity observed for neat PVA and PVA/GO films for *E. coli* bacteria.
- The degradation of PVA-based bioplastics was demonstrated using *B. subtilis* and *P. putida* bacterial strains. The microbial growth suggests that these microorganisms utilized the bioplastic as a carbon source, enabling its breakdown. This process helps achieve a balance between durability and environmental sustainability.
- The soil burial test confirmed the biodegradability of PVA-based bioplastics, highlighting their potential as eco-friendly materials. Additionally, the study revealed that incorporating GO can impact the degradation behavior of the PVA polymer, potentially enhancing its durability and stability for specific applications.

In summary, the successful integration of GO in PVA polymer offers a promising avenue for industrial applications, especially in the packaging sector, where the combination of enhanced mechanical properties, moisture resistance, and antibacterial activity and biodegradability provides significant benefits. However, a thorough and thoughtful approach to industrial scale-up, quality control, and environmental considerations will be essential to realize the full potential of this innovative nanocomposite material.

Bibliography

1. Salgado, P. R., Di Giorgio, L., Musso, Y. S., and Mauri, A. N. Recent developments in smart food packaging focused on biobased and biodegradable polymers. *Frontiers in Sustainable Food Systems*, 5:630393, 2021.

2. Nasiri, S. L., Azizi, M. H., Movahedi, F., Rahimifard, N., and Tavakolipour, H. Potential perspectives of CMC-PET/ZnO bilayer nanocomposite films for food packaging

applications: physical, mechanical and antimicrobial properties. *Journal of Food Measurement and Characterization*, 15(4):3731–3740, 2021.

3. Aznar, M., Ubeda, S., Dreolin, N., and Nerin, C. Determination of non-volatile components of a biodegradable food packaging material based on polyester and polylactic acid (PLA) and its migration to food simulants. *Journal of Chromatography A*, 1583:1–8, 2019.

4. Ahmed, I., Lin, H., Zou, L., Brody, A. L., Li, Z., Qazi, I. M., Pavase, T. R., and Lv, L. A comprehensive review on the application of active packaging technologies to muscle foods. *Food Control*, 82:163–178, 2017.

5. Riano, A. M. S., Vivas, E. M. A., Andrade, H. P. B., Perez, Y. B., Castillo, H. S. V., Daza, L. D., and Real, C. P. V. Physicochemical, structural, and thermal characterization of biodegradable film prepared using arracacha thermoplastic starch and polylactic acid. *Journal of Food Measurement and Characterization*, 16(5):3597–3606, 2022.

6. Abdullah, Z. W., Dong, Y., Davies, I. J., and Barbhuiya, S. PVA, PVA blends, and their nanocomposites for biodegradable packaging application. *Polymer-Plastics Technology and Engineering*, 56(12):1307–1344, 2017.

7. Youssef, H. F., El-Naggar, M. E., Fouda, F. K., and Youssef, A. M. Antimicrobial packaging film based on biodegradable CMC/PVA-zeolite doped with noble metal cations. *Food Packaging and Shelf Life*, 22:100378, 2019.

8. Tao, G., Cai, R., Wang, Y., Song, K., Guo, P., Zhao, P., Zuo, H., and He, H. Biosynthesis and characterization of AgNPs–silk/PVA film for potential packaging application. *Materials,* 10(6): 667, 2017.

9. He, Y., Tian, H., Xiang, A., Ma, S., Yin, D., and Varada Rajulu, A. Fabrication of PVA/GO nanofiber films by electrospinning: application for the adsorption of Cu^{2+} and organic dyes. *Journal of Polymers and the Environment*, 30(7):2964–2975, 2022.

10. Amaregouda, Y., Kamanna, K., and Gasti, T. Biodegradable polyvinyl alcohol/carboxymethyl cellulose composite incorporated with l-alanine functionalized MgO nanoplates: physico-chemical and food packaging features. *Journal of Inorganic and Organometallic Polymers and Materials*, 32(6):2040–2055, 2022.

11. Selvi, J., Mahalakshmi, S., and Parthasarathy, V. Synthesis, structural, optical, electrical and thermal studies of poly(vinyl alcohol)/CdO nanocomposite films. *Journal of Inorganic and Organometallic Polymers and Materials*, 27(6):1918–1926, 2017.

12. Ashfaq, A., Khursheed, N., Fatima, S., Anjum, Z., and Younis, K. Application of nanotechnology in food packaging: Pros and Cons. *Journal of Agriculture and Food*

Research, 7:100270, 2022.

13. Rossa, V., Ferreira, L. E. M., Vasconcelos, S. C., Shimabukuro, E. T. T., Madriaga, V. G. C., Carvalho, A. P., Pergher, S. B. C., Silva, F. C., Ferreira, V. F., Junior, C. A. A., and Lima, T. M. Nanocomposites based on the graphene family for food packaging: historical perspective, preparation methods, and properties. *RSC Advances*, 12(22):14084–14111, 2022.

14. Lin, D., Wu, Z., Huang, Y., Wu, J., Li, C., Qin, W., Wu, D., Li, S., Chen, H., and Zhang, Q. Physical, mechanical, structural and antibacterial properties of polyvinyl alcohol/oregano oil/graphene oxide composite films. *Journal of Polymers and the Environment*, 28(2):638–646, 2020.

15. Ponnamma, D., Yin, Y., Salim, N., Parameswaranpillai, J., Thomas, S., and Hameed, N. Recent progress and multifunctional applications of 3D printed graphene nanocomposites. *Composites Part B: Engineering*, 204:108493, 2021.

16. Cai, D. and Song, M. A simple route to enhance the interface between graphite oxide nanoplatelets and asemi-crystalline polymer for stress transfer. *Nanotechnology*, 20(31):315708, 2009.

17. Xu, Y., Hong, W., Bai, H., Li, C., and Shi, G. Strong and ductile poly(vinyl alcohol)/graphene oxide composite films with a layered structure. *Carbon*, 47(15): 3538–3543, 2009.

18. Xu, C., Shi, L., Guo, L., Wang, X., Wang, X., and Lian, H. Fabrication and characteristics of graphene oxide/nanocellulose fiber/poly(vinyl alcohol) film. *Journal of Applied Polymer Science*, 134(39): 45345, 2017.

19. Sarwar, M. S., Niazi, M. B. K., Jahan, Z., Ahmad, T., and Hussain, A. Preparation and characterization of PVA/nanocellulose/Ag nanocomposite films for antimicrobial food packaging. *Carbohydrate Polymers*, 184:453–464, 2018.

20. Kapila, K., Kirtania, S., Devi, L. M., Saikumar, A., Badwaik, L. S., and Rather, M. A. Potential perspectives on the use of poly (vinyl alcohol)/graphene oxide nanocomposite films and its characterization. *Journal of Food Measurement and Characterization*, 18(2):1012–1025, 2024.

21. Verdejo, R., Bernal, M. M., Romasanta, L. J., and Lopez-Manchado, M. A. Graphene filled polymer nanocomposites. *Journal of Materials Chemistry*, 21(10):3301–3310, 2011.

22. Ma, J., Li, Y., Yin, X., Xu, Y., Yue, J., Bao, J., and Zhou, T. Poly(vinyl alcohol/graphene oxide nanocomposites prepared by in situ polymerization with enhanced

mechanical properties and water vapor barrier properties. *RSC Advances*, 6(55):49448–49458, 2016.

23. Helmiyati, H., Hidayat, Z. S. Z., Sitanggang, I. F. R., and Liftyawati, D. Antimicrobial packaging of ZnO–Nps infused into CMC–PVA nanocomposite films effectively enhances the physicochemical properties. *Polymer Testing*, 104:107412, 2021.

24. Muhamad Fauzi, N. I., Fen, Y. W., Abdullah, J., Kamarudin, M. A., Sheh Omar, N. A., Kamal Eddin, F. B., Md Ramdzan, N. S., and Mohd Daniyal, W. M. E. M. Evaluation of structural and optical properties of graphene oxide-polyvinyl alcohol thin film and its potential for pesticide detection using an optical method. *Photonics*, 9(5):300, 2022.

25. Huang, H. D., Ren, P. G., Chen, J., Zhang, W. Q., Ji, X., and Li, Z. M. High barrier graphene oxide nanosheet/poly(vinyl alcohol) nanocomposite films. *Journal of Membrane Science*, 409–410:156–163, 2012.

26. Taraghi, I., Paszkiewicz, S., Irska, I., Szymczyk, A., Linares, A., Ezquerra, T. A., Kurcz, M., Winkowska-Struzik, M., Lipińska, L., Kowiorski, K., and Piesowicz, E. Thin polymer films based on poly(vinyl alcohol) containing graphene oxide and reduced graphene oxide with functional properties. *Polymer Engineering & Science*, 61(6):1685–1694, 2021.

27. Park, G. T. and Chang, J. H. Comparison of properties of PVA nanocomposites containing reduced graphene oxide and functionalized graphene. *Polymers*, 11(3):450, 2019.

28. Guirguis, O. W., Moselhey, M. T. H., Guirguis, O. W., and Moselhey, M. T. H. Thermal and structural studies of poly (vinyl alcohol) and hydroxypropyl cellulose blends. *Natural Science*, 4(1):57–67, 2011.

29. Lizu, K. M. A., Bari, M. W., Gulshan, F., and Islam, M. R. GO based PVA nanocomposites: tailoring of optical and structural properties of PVA with low percentage of GO nanofillers. *Heliyon*, 7(5):e06983, 2021.

30. Cobos, M., Fernandez, M. J., and Fernandez, M. D. Graphene based poly(vinyl alcohol) nanocomposites prepared by in situ green reduction of graphene oxide by ascorbic acid: influence of graphene content and glycerol plasticizer on properties. *Nanomaterials*, 8(12):1013, 2018.

31. Ebrahimzadeh, S., Ghanbarzadeh, B., and Hamishehkar, H. Physical properties of carboxymethyl cellulose based nano-biocomposites with graphene nano-platelets. *International Journal of Biological Macromolecules*, 84:16–23, 2016.

32. Li, F., Yu, H. Y., Wang, Y. Y., Zhou, Y., Zhang, H., Yao, J. M., Abdalkarim, S. Y. H., and Tam, K. C. Natural biodegradable poly(3-hydroxybutyrate- co-3-hydroxyvalerate) nanocomposites with multifunctional cellulose nanocrystals/graphene oxide hybrids for high-performance food packaging. *Journal of Agricultural and Food Chemistry*, 67(39):10954–10967, 2019.

33. Mahmoudi, N., Ostadhossein, F., and Simchi, A. Physicochemical and antibacterial properties of chitosan-polyvinylpyrrolidone films containing self-organized graphene oxide nanolayers. *Journal of Applied Polymer Science*, 133(11):43194, 2016.

34. Chowdhury, S., Teoh, Y. L., Ong, K. M., Rafflisman Zaidi, N. S., and Mah, S. K. Poly(vinyl) alcohol crosslinked composite packaging film containing gold nanoparticles on shelf life extension of banana. *Food Packaging and Shelf Life*, 24:100463, 2020.

35. Dogan, H. Y., Altin, Y., and Bedeloglu, A. C. Fabrication and properties of graphene oxide and reduced graphene oxide reinforced poly(vinyl alcohol) nanocomposite films for packaging applications. *Polymers and Polymer Composites*, 30:1-11, 2022.

36. Bao, C., Guo, Y., Song, L., and Hu, Y. Poly(vinyl alcohol) nanocomposites based on graphene and graphite oxide: a comparative investigation of property and mechanism. *Journal of Materials Chemistry*, 21(36):13942–13950, 2011.

37. Gautam, S., Sharma, S., Sharma, B., and Jain, P. Antibacterial efficacy of poly (vinyl alcohol) nanocomposites reinforced with graphene oxide and silver nanoparticles for packaging applications. *Polymer Composites*, 42(6):2829–2837, 2021.

38. Hegab, H. M., Elmekawy, A., Zou, L., Mulcahy, D., Saint, C. P., and Markovic, M. G. The controversial antibacterial activity of graphene-based materials. *Carbon*, 105:362–376, 2016.

39. Valentini, F., Calcaterra, A., Ruggiero, V., Pichichero, E., Martino, A., Iosi, F., Bertuccini, L., Antonaroli, S., Mardente, S., Zicari, A., Mari, E., Iovenitti, G., Leone, G., Botta, M., and Talamo, M. Functionalized graphene derivatives: Antibacterial properties and cytotoxicity. *Journal of Nanomaterials*, 1: 2752539, 2019.

40. Chiellini, E., Corti, A., D'Antone, S., and Solaro, R. Biodegradation of poly (vinyl alcohol) based materials. *Progress in Polymer Science*, 28(6):963–1014, 2003.

41. Dhanraj, N. D., Hatha, A. A. M., and Jisha, M. S. Biodegradation of petroleum based and bio-based plastics: approaches to increase the rate of biodegradation. *Archives of Microbiology*, 204(5):1–11, 2022.

42. Abdullah, Z. W. and Dong, Y. Biodegradable and water-resistant poly(vinyl) alcohol (PVA)/starch (ST)/glycerol (GL)/halloysite nanotube (HNT) nanocomposite films for

sustainable food packaging. *Frontiers in Materials*, 6:452153, 2019.

43. Afshar, S. and Baniasadi, H. Investigation the effect of graphene oxide and gelatin/starch weight ratio on the properties of starch/gelatin/GO nanocomposite films: The RSM study. *International Journal of Biological Macromolecules*, 109:1019–1028, 2018.